Kinetics and Modeling of the H_2—O_2—NO_x System

J. H. BROMLY and F. J. BARNES
SECWA (Alinta Gas), Perth, Western Australia

P. F. NELSON
CSIRO Division of Coal and Energy Technology, North Ryde, New South Wales

B. S. HAYNES*
Department of Chemical Engineering, University of Sydney, New South Wales, Australia

Abstract

The addition of NO (0 to 400ppm) to mixtures of H_2 (ca. 1%) and O_2 (0.7 to 22%) has been studied over the temperature range 700 to 825 K, in a flow reactor at atmospheric pressure. The overall effect of NO is to promote the oxidation of H_2 but high concentrations of O_2 actually inhibit the NO-promoted oxidation of H_2.

A detailed kinetic mechanism has been constructed and found to describe the experimental observations. The promotion of the oxidation of H_2 arises through the catalytic cycle

$$H + O_2 + M \Longleftrightarrow HO_2 + M \qquad \text{R.5}$$

$$NO + HO_2 \Longleftrightarrow NO_2 + OH \qquad \text{R.34}$$

$$NO_2 + H \Longleftrightarrow NO + OH \qquad \text{R.35}$$

$$H_2 + OH \Longleftrightarrow H_2O + H \qquad \text{R.2}$$

The ability of R.34 to reactivate chains normally terminated by the formation of HO_2 is a key feature of this system.

The predictions are highly sensitive to the rate of the reaction R.5 and the rate constants for this reaction is the only adjustable parameter required in the model. The value of $k_{5,N2}$ found to describe all the results

$$k_{5,N2} = 2.60 \times 10^{15} \exp(+1350 \text{ cal.mol}^{-1}/RT) \text{ cm}^6.\text{mol}^{-2}.\text{s}^{-1}$$

has an absolute uncertainty <35%. The uncertainty relative to other important rate constants in the H_2—O_2 system is less than 10%.

Introduction

Low concentrations of various fuels promote the oxidation of NO to NO_2 in the presence of oxygen at temperatures as low as 330°C [1–5]. This phenomenon is believed to contribute to the emission of NO_2 from combustion appliances which give rise to conditions where O_2, NO, and unburned fuel, including CO and H_2, may coexist. Such appliances include domestic gas cookers and heaters [2,3] and gas turbine exhausts.

The influence of the oxides of nitrogen (NO and NO_2) on promoting the ignition of H_2/O_2 mixtures is also profound and has long been recognized [6–11]. The

*To whom correspondence should be addressed.

International Journal of Chemical Kinetics, Vol. 27, 1165–1178 (1995)
 CCC 0538-8066/95/121165-14

basic mechanism appears to be remarkably simple, with reactions R.34 and R.35 effectively turning HO_2-formation (by R.5) into a chain-propagating rather than chain-terminating process:

$$H + O_2 + M \Longleftrightarrow HO_2 + M \qquad \text{R.5}^1$$

$$NO + HO_2 \Longleftrightarrow NO_2 + OH \qquad \text{R.34}$$

$$NO_2 + H \Longleftrightarrow NO + OH \qquad \text{R.35}$$

$$H_2 + OH \Longleftrightarrow H_2O + H \qquad \text{R.2}$$

The rates of reactions R.2, R.34 [12], and R.35 [13] are well established over a wide range of temperatures, but there remains considerable uncertainty in the rate of R.5 in the range of temperatures relevant to low-temperature ignition phenomena. Experimental determinations [8,14–16] and recommendations [11,18–22] for the value of k_5 (M = N_2, T = 750 K) range from 3.2 to 9.6 × 10^{15} $cm^6.mol^{-2}.s^{-1}$. Given the very high sensitivity of ignition calculations to the value of this rate constant [9,10], this range of uncertainty seriously limits the modelling of such systems.

This article reports an experimental and modelling study of the H_2—O_2 reaction sensitized by NO. The objective here is to develop a detailed kinetic model capable of describing the observed behavior in order to shed more light on the value of k_5 at temperatures around 750 K and to provide a basis on which to construct models of the more complicated mutually sensitized reactions of NO and hydrocarbons.

Experimental

The experimental apparatus has been described previously [2,3]. The reaction was carried out at atmospheric pressure in a laminar-flow reactor consisting of 3 m × 18 mm ID uncoated pyrex tubing. The reactor was housed within an electrically-heated, fan-stirred oven which provided constant and uniform temperatures (±0.5°C). The maximum temperature achievable with the pyrex reactor was 825 K.

The reaction mixtures were made by combining separately metered streams of nitrogen, oxygen (or air), hydrogen, and NO (1% in N_2). The flowrates of the various streams were determined, ±1%, at each setting, using a Buck M5 soap-film calibrator.

The nitrogen and oxygen (or air) streams were combined and introduced into the reactor via a preheating section located within the oven. This preheating section, which consisted of a 6m length of 4mm id aluminum tubing and a 2l reservoir, ensured that the major flow entered the reactor within 1 °C of the kiln control temperature.

The combined NO + H_2 stream was partially preheated and was injected into the main stream at the entrance to the reactor via an axial countercurrent jet in order to promote mixing between the streams. The injection point was located immediately upstream of a constriction which served to promote further mixing. The flowrate of the injected stream was less than 5% of the air flowrate. No differences in the results obtained could be detected if the NO was premixed with the O_2/N_2 stream rather than with the H_2 stream.

The reactor was fitted with three sampling points, located 1m, 2m, and 3m downstream of the mixing point to allow a range of residence times to be investigated.

[1] The reaction identification numbers are as given in Table I.

The residence time of the reaction mixture at the ports could also be varied by varying the gas flowrates entering the reactor. Gas samples drawn through the various offtakes were piped to the exterior of the kiln through narrow-bore pyrex tubing (3 mm id). The sample flowrate was typically 25% of the total reactant flow rate. Outside the kiln, teflon tubing was used for all sample lines.

Nitrogen oxides were determined by a conventional chemiluminescence analyzer equipped with a stainless-steel converter. Hydrogen was determined routinely (±5%) by flammable gas detector and by gas chromatography (±2%); O_2 was determined using a fuel-cell detector. For detection of H_2O concentrations above about 0.1%, a relative humidity sensor was used; lower concentrations were measured with a thick-film dewpoint sensor. Both sensors were calibrated against H_2O/N_2 mixtures generated by mixing dry N_2 with a second N_2 stream which had been saturated by bubbling through a water bath. The water concentrations reported here are accurate ±20% above 1000 ppm; ±30% in the range 100 to 1000ppm.

Computer-kinetic modelling of the reactions was carried out using the Sandia SENKIN/CHEMKIN II package [23,24]. All reactions were treated as reversible, with reverse rates being calculated from the forward rates and the Sandia thermodynamic database [25].

Results

Results were obtained for the reaction of ca. 0.8% H_2 with O_2 (0.7 to 22%) in the presence of NO (0 to 400 ppm), at temperatures in the range from 690 to 825 K. The residence time of the reaction mixture was varied in the range 1 to 5.5 s. For all of the conditions examined, there was no detectable reaction of H_2 with O_2 unless NO or NO_2 was also present in the reaction gases. The consumption of H_2 observed in the presence of the nitrogen oxides ranges from 0 to 100%, depending on the specific conditions. Washing of the reactor with either acid or KCl solution had no significant effect on the products of reaction at 750 K.

Figure 1 shows the results for 0.8% H_2 reacting for 3.2 s at 750 K with 2.9% and 10% O_2, in the presence of inlet NO concentrations up to 400 ppm. In both cases, at low levels of NO addition, all the NO is converted to NO_2 without substantial consumption of H_2. At higher levels of NO addition, $[NO_2]$ reaches a plateau level (higher for greater $[O_2]$) which is maintained even at very high inlet NO concentrations. The onset of significant oxidation of H_2 coincides with the departure of the $[NO_2]$ curve from 100% conversion of NO and the onset of the plateau region but H_2O production begins to decrease at some point after the $[NO_2]$ plateau is established.

The influence of $[O_2]$ on the products from 0.92% H_2 + 27 ppm NO at 825 K is shown in Figure 2. The extent of oxidation of H_2 is greatest at slightly lean conditions but is suppressed as the O_2 concentration is increased. The conversion of NO to NO_2 is low under the most reactive conditions for H_2 oxidation but increases approximately linearly with $[O_2]$. At sufficiently high $[O_2]$, there is practically complete conversion $NO \rightarrow NO_2$ and further increases in $[O_2]$ do not affect $[NO_2]$. The different regions in Figures 1 and 2 can be considered qualitatively in terms of the inlet $[O_2]/[NO]$ ratio-high values of this ratio lead to complete conversion of the NO whereas low values give rise to the NO_2-plateaus in Figure 1 and the NO_2-ramp in Figure 2.

The formation of products as a function of residence time in the reactor at 825 K is shown in Figure 3. The conversion of NO to NO_2 occurs on a shorter timescale than H_2 oxidation. This effect is particularly apparent at lower temperatures when complete

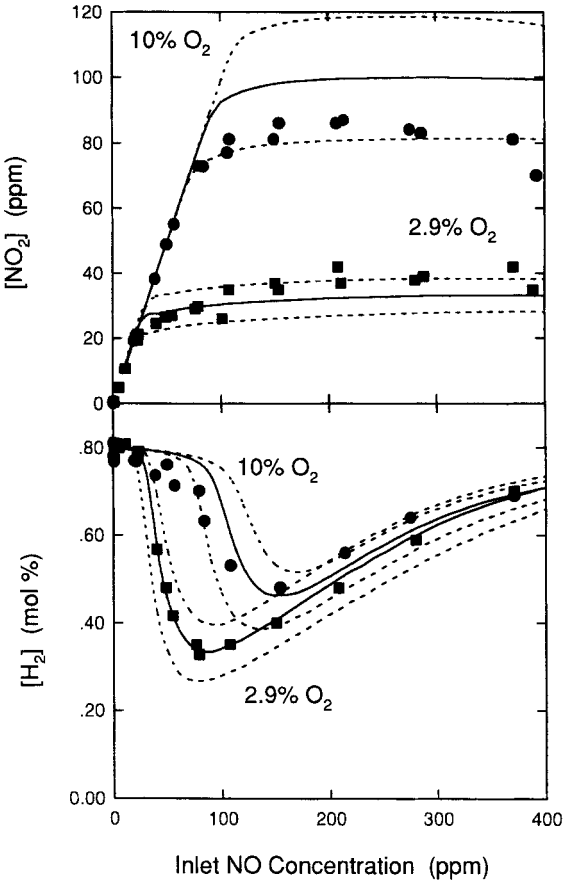

Figure 1. Products of the atmospheric-pressure reaction of 0.80% H_2 with O_2 ((■) 2.9% O_2; (●) 10.0% O_2) in the presence of NO. Reactor temperature 750 K, residence time 3.2 s. The solid lines show the predictions of the model given in Table I; the dotted lines show the predictions obtained when k_5 is varied ±20%.

conversion NO → NO_2 occurs before H_2 consumption is detectable. Also apparent in Figure 3 is the fact that [NO_2] reaches a steady value, which does not vary even as H_2O formation continues and NO remains unconverted.

At temperatures around 700 K, there is significantly less reaction of H_2 and the system becomes very sensitive to temperature. Figure 4 shows the results obtained for NO additions to 0.8% H_2 + 2.6% O_2 at 710 K. As the NO inlet concentration is increased, the NO_2 concentration increases and then approaches a plateau value similar to that observed at 750 K in Figure 1. Now, however, at higher levels of NO addition, [NO_2] begins to fall. The consumption of hydrogen in the experiments at 710 K and lower was insufficient to be measured accurately.

Discussion

The occurrence of a characteristic plateau value of [NO_2] in the NO_x-sensitized H_2/O_2 reaction was first reported by Ashmore and Tyler [8] and was exploited by

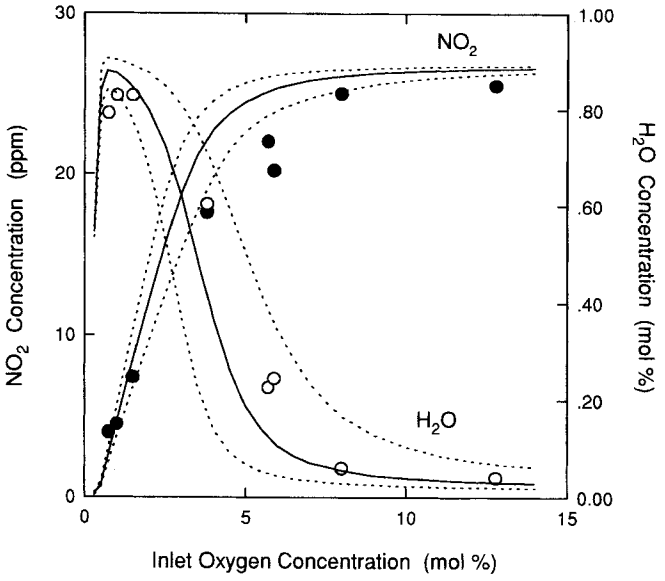

Figure 2. Formation of NO_2 (●) and H_2O (○) in the reaction, at atmospheric pressure, of 0.92% H_2 with O_2 in the presence of 27 ppm NO. Reactor temperature 825 K, residence time 2.8 s. The solid lines show the predictions of the model given in Table I; the dotted lines show the predictions obtained when k_5 is varied ±20%.

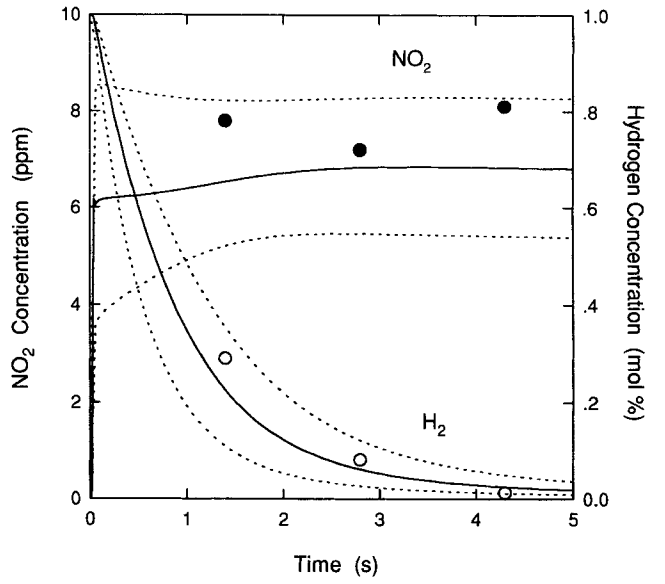

Figure 3. Time-resolved profiles of $[NO_2]$ (●) and $[H_2]$ (○) in the reaction of 1.0% H_2 with 1.3% O_2, in the presence of 19 ppm NO. Reactor temperature 825 K, residence time 2.8 s. The solid lines show the predictions of the model given in Table I; the dotted lines show the predictions obtained when k_5 is varied ±20%.

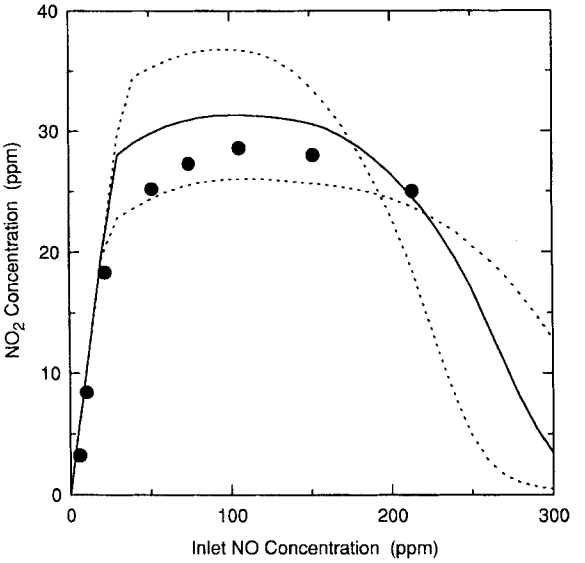

Figure 4. Formation of NO_2 in the atmospheric-pressure reaction of 0.80% H_2 with 2.6% O_2 in the presence of NO. Reactor temperature 710 K, residence time 3.5 s. The solid lines show the predictions of the model given in Table I; the dotted lines show the predictions obtained when k_5 is varied ±20%.

them to yield an estimate of k_5. They pointed out that reactions R.5, R.34, R.35, and 2 × R.2 constitute a catalytic cycle which, while H_2 and O_2 remain unconsumed, tends towards a pseudo-steady-state condition characterized by a constant concentration of NO_2, given by eq. 1 [8]:

$$[NO_2]_{plateau} = \frac{k_5[M]}{k_{35}}[O_2] \tag{1}$$

If the total concentration of NO_x is less than the plateau level indicated by eq. (1), the NO_x is substantially converted to NO_2, $[NO_2] \rightarrow [NO_x]$, otherwise $[NO_2] \rightarrow [NO_2]_{plateau}$. This simple picture describes qualitatively the NO_2 profiles seen, for example, in Figure 1. However, in order to extend the analysis to the whole range of $[NO_2]$ and to include analysis of the H_2 and H_2O profiles as well, we have investigated the kinetics of the system by detailed computer modelling.

Table I provides the details of the mechanism constructed for the kinetic analyses. Reactions 1 to 24 describe the H_2—O_2 system in the usual way. For the H/N/O system, reactions 25 to 37 are the conventional choices for combustion systems [20]; reaction 38 may become significant at high NO concentrations. Previous work on the $H_2/O_2/NO_x$ system [3,8–10] suggested the need to include the reactions of nitrous acid, HONO, reactions 39–44. For completeness, some reactions of nitric acid ($HONO_2$), NO_3, and O_3 (reactions 45–64) were included although these were subsequently found to have no significant influence under the present conditions. However, calculations did show that these reactions do become important at lower temperatures or under strongly inhibited conditions (close to extinction).

In choosing rate constants for the various reactions, preference was given to values recommended for the temperatures around 750 K. This frequently presented

TABLE I. Reaction mechanism for the H_2—NO_x—O_2 system, $k = AT^n exp(-E/RT)$ in units cal, cm^3, mol, and s. Three-body recombination reaction in the fall-off region are calculated from the high- and low-pressure limits using either the Lindemann or Troe procedures. In the latter case, the characteristic factor F_c is calculated as $F_c = exp(-T^{***}/T)$.

		A	n	E	Ref.
1.	$H_2 + O_2 = 2OH$	1.70E + 13	0.0	47780	[20]
2.	$OH + H_2 = H_2O + H$	2.14E + 08	1.5	3449	[26]
3.	$H + O_2 = OH + O$	1.00E + 14	0.0	14850	[26]
4.	$O + H_2 = OH + H$	5.00E + 04	2.7	6290	[26]
5.	$H + O_2 + M = HO_2 + M$	2.60E + 15	0.0	−1350	this work
	Enhancement Factors $H_2O = 12$	$H_2 = 1.82$	$O_2 = 0.60$		[8]
6.	$OH + HO_2 = H_2O + O_2$	2.89E + 13	0.0	−497	[22]
7.	$H + HO_2 = 2OH$	1.69E + 14	0.0	874	[22]
8.	$H + HO_2 = H_2 + O_2$	4.28E + 13	0.0	1411	[22]
9.	$H + HO_2 = H_2O + O$	3.01E + 13	0.0	1721	[22]
10.	$O + HO_2 = O_2 + OH$	3.25E + 13	0.0	0	[22]
11.	$2OH = O + H_2O$	4.33E + 03	2.7	−2485	[26]
12.	$H + H + M = H_2 + M$	1.00E + 18	−1.0	0	[20]
	Enhancement Factors $H_2O = 0$	$H_2 = 0$			
13.	$H + H + H_2 = H_2 + H_2$	9.20E + 16	−0.6	0	[20]
14.	$H + H + H_2O = H_2 + H_2O$	6.00E + 19	−1.3	0	[20]
15.	$H + OH + M = H_2O + M$	1.60E + 22	−2.0	0	[20]
	Enhancement Factors $H_2O = 5$				
16.	$H + O + M = OH + M$	6.20E + 16	−0.6	0	[20]
	Enhancement factors $H_2O = 5$				
17.	$O + O + M = O_2 + M$	1.89E + 13	0.0	−1788	[20]
18.	$HO_2 + HO_2 = H_2O_2 + O_2$	4.20E + 14	0.0	12000	[12]
19.	$HO_2 + HO_2 = H_2O_2 + O_2$	1.30E + 11	0.0	−1630	[12]
20.	$H_2O_2 + M = OH + OH + M$	1.21E + 17	0.0	45507	[22]
21.	$H_2O_2 + H = HO_2 + H_2$	1.69E + 12	0.0	3756	[22]
22.	$H_2O_2 + H = H_2O + OH$	1.02E + 13	0.0	3577	[22]
23.	$H_2O_2 + OH = H_2O + HO_2$	7.83E + 12	0.0	1331	[22]
24.	$H_2O_2 + O = HO_2 + OH$	6.62E + 11	0.0	3974	[22]
25.	$H + NO + M = HNO + M$	1.17E + 18	−0.9	0	[27]
	Enhancement Factors $H_2O = 10$	$H_2 = 2$	$O_2 = 2$	$N_2 = 2$	[20]
26.	$HNO + O_2 = NO + HO_2$	2.20E + 10	0.0	9140	[28]
27.	$HNO + OH = NO + H_2O$	1.30E + 07	1.9	−956	[29]
28.	$HNO + H = H_2 + NO$	5.00E + 12	0.0	0	[20,30]
29.	$HNO + O = OH + NO$	1.10E + 13	0.0	0	[31]
30.	$HNO + HNO = H_2O + N_2O$	9.00E + 08	0.0	3080	[32]
31.	$N + NO = N_2 + O$	3.27E + 12	0.3	0	[20]
32.	$N + O_2 = NO + O$	6.40E + 09	1.0	6280	[20]
33.	$N + OH = NO + H$	3.80E + 13	0.0	0	[20]
34.	$HO_2 + NO = NO_2 + OH$	2.23E + 12	0.0	−477	[12]
35.	$NO_2 + H = NO + OH$	1.32E + 14	0.0	360	[13]
36.	$NO_2 + O = NO + O_2$	1.00E + 13	0.0	600	[20]
37.	$NO + O(+M) = NO_2(+M)$	3.26E + 12	0.3	0	[21]
	Low pressure limit ($T^{***} = 1850$ K)	3.33E + 20	−1.6	0	[21]
38.	$NO + NO + O_2 = NO_2 + NO_2$	1.20E + 09	0.0	−1050	[21]
39.	$NO + OH(+M) = HONO(+M)$	1.93E + 13	0.0	0	[21]
	Low pressure limit ($T^{***} = 1300$ K)	2.33E + 23	−2.4	0	
40.	$H + NO_2 + M = HONO + M$	1.40E + 18	−1.5	900	[33]
41.	$H_2 + NO_2 = H + HONO$	1.20E + 13	0.0	29000	[34]
42.	$HONO + OH = H_2O + NO_2$	1.69E + 13	0.0	−260	[35]

(Continued)

TABLE I. (Continued)

		A	n	E	Ref.
43.	$HONO + O = OH + NO_2$	1.00E + 12	0.0	0	est.
44.	$HONO + HONO = H_2O + NO_2 + NO$	2.30E + 12	0.0	8350	[32]
45.	$HO_2 + NO + M = HONO_2 + M$	2.23E + 12	−3.5	2200	[33]
46.	$NO_2 + OH(+ M) = HONO_2 (+M)$	3.61E + 13	0.0	0	[21]
	Low pressure limit	1.44E + 25	−2.9	0	
47.	$HONO_2 + OH = H_2O + NO_3$	1.03E + 10	0.0	−1240	[36]
48.	$NO_3 + OH = HO_2 + NO_2$	1.39E + 13	0.0	0.0	[21]
49.	$NO_3 + O = O_2 + NO_2$	1.02E + 13	0.0	0.0	[21]
50.	$NO_3 + H = NO_2 + OH$	6.00E + 13	0.0	0	[36]
51.	$NO_3 + HO_2 = O_2 + HONO_2$	5.60E + 11	0.0	0	[36]
52.	$NO_3 + HO_2 = O_2 + NO_2 + OH$	2.00E + 12	0.0	0	[36]
53.	$NO_3 + NO_3 = NO_2 + NO_2 + O_2$	5.12E + 11	0.0	4840	[36]
54.	$NO_3 + M = O_2 + NO + M$	2.05E + 08	1.0	12122	[36]
	Enhancement Factors $NO_2 = 0$				
55.	$NO_3 + NO_2 = NO + NO_2 + O_2$	3.25E + 10	0.0	2960	[36]
56.	$NO_3 + NO = NO_2 + NO_2$	1.08E + 13	0.0	−219	[21]
57.	$NO_2 + O(+M) = NO_3(+M)$	1.21E + 13	0.0	0	[21]
	Low pressure limit (T^{***} = 1300 K)	2.94E + 21	−2.0	0	[21]
58.	$NO_2 + O_3 = NO_3 + O_2$	7.23E + 10	0.0	4870	[21]
59.	$O + O_2 + M = O_3 + M$	1.88E + 21	−2.8	0	[21]
60.	$O + O_3 = O_2 + O_2$	4.80E + 12	0.0	4090	[21]
61.	$H + O_3 = OH + O_2$	8.43E + 13	0.0	950	[21]
62.	$OH + O_3 = HO_2 + O_2$	1.14E + 12	0.0	2000	[21]
63.	$NO + O_3 = NO_2 + O_2$	1.08E + 12	0.0	2720	[21]
64.	$HO_2 + O_3 = OH + O_2 + O_2$	8.43E + 09	0.0	1200	[21]

a dilemma as this temperature falls between the ranges of interest for atmospheric chemistry and combustion chemistry. However, except where discussed below, the predictions of the reaction behavior were insensitive to uncertainties in the values of rate constants.

The solid lines in Figures 1 to 4 represent the predictions of the model. Residence times were calculated from the known gas velocity and the length from the reactant mixing point to the sample offtake. For comparison with the experimental NO_2 profiles, the predictions for [HONO] and [NO_2] have been summed and expressed as NO_2, since the stainless-steel converter employed in the chemiluminescent analyzer could not distinguish between these species. However, it should be noted that the predicted concentrations of HONO were never greater than about 10% of [NO2], and often much less than that.

All the predictions were obtained with the rate constants shown in Table I. With the exception of the value for $k_{5,N2}$, all those rate constants were taken from the literature without adjustment. The value of $k_{5,N2}$ which was used to generate the predictions was

$$k_{5,N_2} = 2.60 \times 10^{15} \exp(+1350/RT) \qquad cm^6.mol^{-2}.s^{-1}$$

The temperature dependence is that of Hsu et al. [15] and is discussed below. The relative efficiencies of other collision partners were taken from the work of Ashmore and Tyler [8] because that work was carried out under conditions similar to those employed here. For O_2, the collision efficiency relative to N_2 is therefore $\gamma = 0.60$.

While Miller and Bowman [20] recommend $\gamma = 0.77$, this discrepancy introduces very little (<5%) uncertainty into the modelling as the maximum O_2 mole fraction employed in the present work was 0.22. Similarly, the considerable uncertainty in the relative collision efficiency of H_2O [8,11,14,15,20] is not important because the low concentration of this species (mole fraction <0.008) makes the calculations insensitive to this value.

Figure 5 shows the normalized mole fraction sensitivity coefficients ($S_{ij} = \partial lnx_i/\partial lnA_j$) for the predictions of $[NO_2]$ and $[H_2O]$ with respect to the values of the individual rate constants for the reaction conditions corresponding to Figure 1. The predicted profiles for $[NO_2]$ under reactive conditions are sensitive to only two rate coefficients, with $S_{NO2.5} \rightarrow +1$ and $S_{NO2.35} \rightarrow -1$ in the plateau region, in accordance with the form of eq. (1). Therefore, based on the matching of the $[NO_2]$ profiles alone, we may conclude that the ratio $k_{5,N2}/k_{35} = 63 \pm 10$ cm^3.mol^{-1} at 750 K. Since the value for k_{35} is known very accurately (±20% [13]) in the temperature range of the present work, an absolute uncertainty <35% may be ascribed to our value of $k_{5,N2}$.

When the matching of the $[H_2]$ and $[H_2O]$ profiles is considered, the predictions are again very sensitive to the values of k_5, and, under some circumstances, to k_{35}. However the sensitivities to these rate constants are no longer equal and opposite

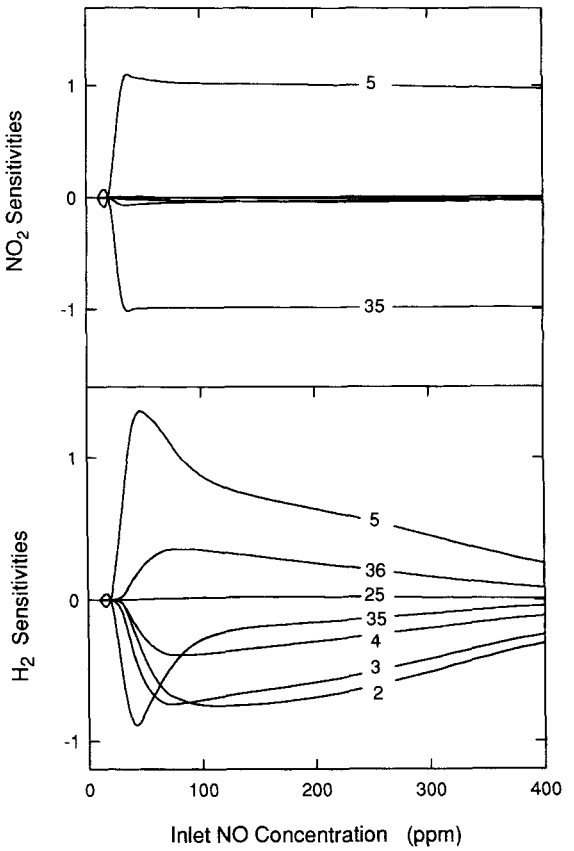

Figure 5. Model sensitivity coefficients ($S_{ij} = \partial lnx_i/\partial lnA_j$) for the formation of NO_2 and H_2O under the conditions shown in Figure 1 (2.9% O_2 + 0.8% H_2 at 750 K, $\tau = 3.2$ s.).

and, as shown in Figure 5, there are regions where the predictions are substantially independent of k_{35}. This behavior allows the value of k_5 to be assessed independently of k_{35}, but still in terms of the controlling rate constants, chiefly those for the chain-branching reactions 2 and 3. While the various sensitivity coefficients for the formation of H_2O vary substantially, depending on the reaction conditions and the extent of conversion, the excellent fit to the data under conditions exhibiting high sensitivity to the values of the rate constants confirms the accuracy of our value of $k_{5,N2}$ relative to the values of k_2 and k_3 in particular. Since the rates of these reactions are known within ±30% [26], the ability of the model to describe the $[H_2O]$ and $[H_2]$ profiles provides an independent verification of the absolute accuracy of the value of $k_{5,N2}$ used in this work.

Around 700 K, there is much less reactivity of H_2, but the model continues to describe the observations of $[NO_2]$. The sensitivity coefficients for NO_2 at 710 K (Fig. 4) are shown in Figure 6. At low values of NO addition, the sensitivities are precisely as described above. However at higher inlet NO concentrations, where the measurements and the predictions for $[NO_2]$ show a fall-off from the plateau, the rate constants of other reactions become progressively more important in determining $[NO_2]$. This situation arises because the overall reactivity of the system is inhibited by high concentrations of NO and the production of radicals is so weak that there is barely sufficient consumption of H_2 to establish the steady state described by eq. (1). Under these conditions the NO_2 concentration becomes dependent on the rate constants governing the rate of oxidation of the hydrogen itself.

For the runs at 825 K, the system approaches criticality and depends to some extent also on the reactions of the HO_2 radical (R.6–8 in particular). Nevertheless, the $[H_2]$ profiles are accurately modelled under these conditions also.

The influence on the model predictions of possible heterogeneous losses of reactive species such as $HO_2 \rightarrow$ wall and $H \rightarrow$ wall was examined. The equivalent homogeneous first-order rate constant for the mass-transfer-limited loss of radical species (H, OH,

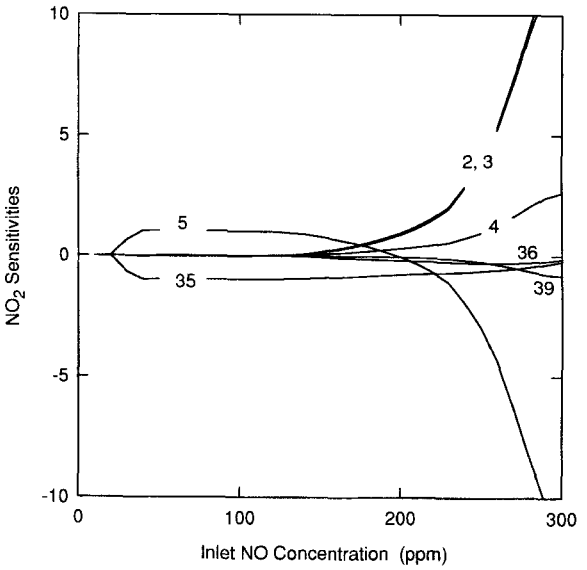

Figure 6. Model sensitivity coefficients ($S_{ij} = \partial ln x_i / \partial ln A_j$) for the formation of NO_2 under the conditions shown in Figure 4 (2.6% O_2 + 0.8% H_2, at 710 K, τ = 3.2 s.).

O, and HO_2) at the wall was included in the model ($k = 20\ s^{-1}$ for HO_2; $k = 30\ s^{-1}$ for O and OH; and $k = 100\ s^{-1}$ for H) to simulate the maximum possible influence of such heterogeneous losses. Figure 7 shows that, for the typical conditions of 0.8%H_2 + 2.6% O_2 + 100 ppm NO, these heterogeneous losses must be negligible at temperatures >720 K for hydrogen consumption, or >700 K for NO_2 formation. This is in accordance with the lack of influence of either KCl- or HCl washing of the reactor on the results (at 750 K); and with the ability of the model to describe, without adjustment, all the experimental observations over the range of conditions studied.

It is interesting to note that, although the rate of consumption of H_2 is enormously accelerated by the ability of the NO/NO_2 cycle to reactivate HO_2, the system does not necessarily proceed to ignition. The reason for this lies in the occurrence of other chain-terminating processes which limit the growth in the radical pool, these processes include reactions R.25, R.36, and R.39:

$$H + NO + M \Longleftrightarrow HNO + M \qquad \text{R.25}$$

$$NO_2 + O \Longleftrightarrow NO + O_2 \qquad \text{R.36}$$

$$OH + NO + M \Longleftrightarrow HONO + M \qquad \text{R.39}$$

The inhibition of the hydrogen reaction at high levels of NO addition is largely the result of the radical-scavenging role of NO by R.25 and R39. The inhibition of the mutual sensitization of the oxidation of NO and *n*-butane at high [NO] has also been attributed to the occurrence of R.39 [3] as subsequent reactions of HONO are most likely to remove further radicals, eg., R41–43. Reaction 25 is particularly important

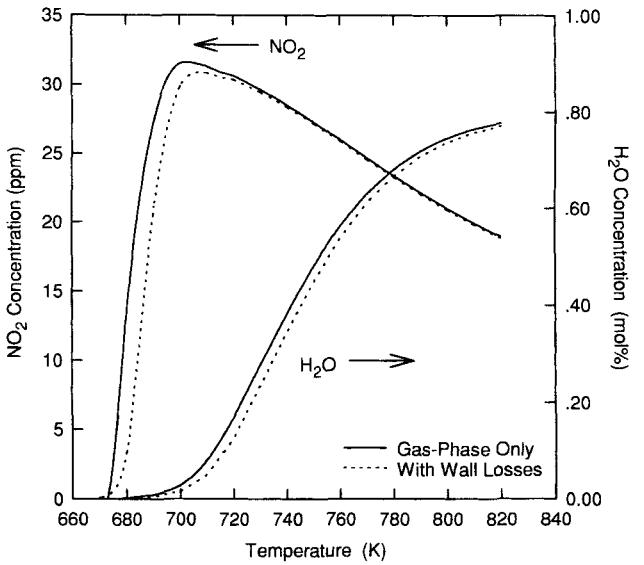

Figure 7. Comparison between predicted results for [NO_2] and [H_2O] showing the effect of including heterogeneous wall losses of radicals (O, H, OH, and HO_2) in the homogeneous mechanism described in Table I. The solid lines show the results for homogeneous reaction only while the dotted lines show the predictions with mass-transfer limited wall loss rates of the radicals. The reaction conditions are 2.6% O_2 + 0.8% H_2 + 100 ppm NO, τ = 3.2 s.

in rich and near-stoichiometric mixtures but, under leaner conditions, the oxidation of HNO (R.26, 29) is radical-producing and R.25 ceases to be a net termination step.

Reaction R.36 is always important as a chain terminator. In particular, the inhibition of hydrogen consumption at high concentrations of O_2, as shown in Figure 2 is largely the result of radical consumption by R.36 because higher concentrations of both O atoms and of NO_2 are favored under oxygen-rich conditions.

The possibility that further radical removal might occur via the reaction

$$NO_2 + HO_2 \Longleftrightarrow HONO + O_2$$

needs to be considered. There have been numerous references [37–39] to the occurrence of this process in studies of the formation kinetics of pernitric acid (HO_2NO_2) at subambient temperatures, but estimates of the rate constant have varied widely. The existence of this channel has, however, been rejected recently by Jemi-Alade and Thrush [39]. If this process is included in our model with a rate constant of the order of 10^{11} $cm^3.mol^{-1}.s^{-1}$ [37], it is found to provide strong inhibition of the H_2 reaction, inconsistent with the experimental results. Therefore, the reaction has been excluded from the present model.

The success of the present model under high-sensitivity conditions suggests that the internal consistency of the rate constants for reactions R.2, 3, 4, and 35 is much better than their established absolute accuracies. No one of these rate constants could be varied by more than 10% without requiring adjustments in one or more of the others. Given the values of k_2, k_3, k_4, and k_{35} employed in the model, the uncertainty in our value for $k_{5,N2}$ is $\pm 15\%$.

Figure 8 compares our results for $k_{5,N2}$ with experimental values reported by others. The data are presented in Arrhenius form because recent direct measurements of this rate constant over wide temperature ranges have suggested this is preferable to the T^n form [14,15]. Our results agree very well with those of Hsu et al. [15] but are not at all consistent with the values reported by Carleton et al. [14]. The reason for the discrepancy between the values of Carleton et al. [14] and Hsu et al. [15] is not obvious because both groups used very similar direct measurement techniques, but, on the basis of our results, the results of Hsu et al. [15] should be preferred.

The values reported by Hanning–Lee et al. [17] were obtained from a kinetic study of H_2—O_2 systems close to ignition and are too widely scattered to be considered reliable. The value attributed to Ashmore and Tyler [8], in reasonable agreement with our results, is derived from their value for k_5/k_{35} obtained from measurements of $[NO_2]_{plateau}$ (eq. 1) in H_2—O_2—NO mixtures in static vessels.

The higher-temperature results of Slack [16] pertain to a computer-kinetic analysis of induction times in shock-heated H_2—O_2 mixtures and are somewhat model-dependent. In particular, rate constants chosen for the reactions 2, 3, and 4, as well as for competing reactions of HO_2, especially R.7, may influence such an analysis and the real uncertainty limits on Slack's [16] results must be substantially larger than the quoted $\pm 20\%$ but Slack does not give enough details on parametric sensitivities to allow a more realistic estimate to be made.

Conclusion

The addition of NO to H_2—O_2 mixtures strongly promotes the consumption of H_2 in excess O_2 at temperatures in a flow reactor in the range 690 to 825 K and leads to the formation of NO_2. A detailed kinetic model of the H_2—O_2 system, when coupled

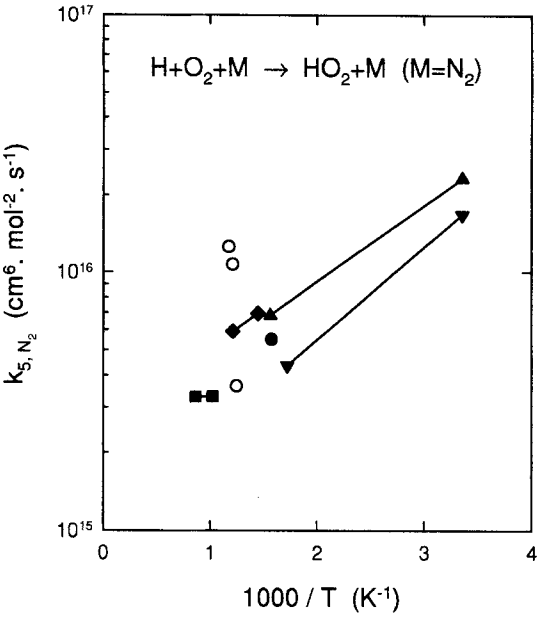

Figure 8. Comparison of rate constants for $k_{5,N2}$ (H + O_2 + M → HO_2 + M, M = N_2) from: (◆) this work; (▲) Hsu et al. [15]; (▼) Carleton et al. [14]; (○) Hanning-Lee et al. [17]; (●) Ashmore and Tyler [8]; and (■) Slack [16].

with a description of the NO/NO_2 chemistry relevant to low-temperature ignition temperatures, describes all the observations accurately, including the inhibition of the system by O_2.

The predictions are highly sensitive to the rate of the reaction R.5

R.5 $$H + O_2 + M \longrightarrow HO_2 + M$$

and the rate of this reaction is the only adjustable parameter required in the model. The value of $k_{5,N2}$ found to describe all the results ($k_{5,N2} = 2.60 \times 10^{15} \exp(1350/RT)$ $cm^6.mol^{-2}.s^{-1}$) agrees well with earlier determinations and is believed to have an absolute uncertainty <35%. The uncertainty relative to other rate constants in the H_2—O_2 system is probably less than 10%.

Acknowledgment

This work is supported in major part by a Collaborative Grant from the State Energy Commission of Western Australia (SECWA [now Alinta Gas]) and the Australian Research Council.

Bibliography

[1] D. Jaasma and G. Borman, *Combust. Sci. Tech.*, **23,** 83 (1980).

[2] J.H. Bromly, *The Formation of Nitrogen Oxides in Gas Combustion,* Ph.D. Thesis, Murdoch University, 1991.

[3] J. H. Bromly, F. J. Barnes, R. Mandyczewsky, T. J. Edwards, and B. S. Haynes, in *Twenty Fourth Symposium (International) on Combustion,* The Combustion Institute, Pittsburgh Pennsylvania, 1992, pp. 899–907.

[4] M. Hori, N. Matsunaga, P. C. Malte, and N. M. Marinov, in *Twenty Fourth Symposium (International) on Combustion,* The Combustion Institute, Pittsburgh, Pennsylvania, 1992, pp. 909–916.
[5] F. J. Barnes, J. H. Bromly, R. Mandyczewsky, T. J. Edwards and B. S. Haynes, in *International Gas Research Conference Preprints,* 1992, Vol. IV, p. 257.
[6] H. W. Thompson and C. N. Hinshelwood, *Proc. Roy. Soc. Lond.,* **A124,** 219 (1928).
[7] F. S. Dainton and R. G. W. Norrish, *Proc. Roy. Soc. London,* **A177,** 393 (1941).
[8] P. G. Ashmore and B. J. Tyler, *Trans. Farad. Soc.,* **58,** 1108 (1962).
[9] M. Slack and A. Grillo, *Investigation of Hydrogen-Air Ignition Sensitised by Nitric Oxide and by Nitrogen Dioxide,* NASA Report CR-2896, 1977.
[10] W. A. Laster and P. E. Sojka, *J. Propuls.* **5,** 510 (1989).
[11] G. Dixon-Lewis and D. J. Williams, in *Comprehensive Chemical Kinetics,* C. H. Bamford and C. F. H. Tripper, Eds, Elsevier Scientific, Amsterdam, 1977, Vol. 17, p. 1.
[12] T. J. Wallington, P. Dagaut, and M. J. Kurylo, *Chem. Rev.,* **92,** 667 (1992).
[13] T. Ko and A. Fontijn, *J. Phys. Chem.,* **95,** 3984 (1991).
[14] K. L. Carleton, W. J. Kessler, and W. J. Marinelli, *J. Phys. Chem.,* **97,** 6412 (1993).
[15] K.-J. Hsu, S. M. Anderson, J. L. Durant, and F. Kaufman, *J. Phys. Chem.,* **93,** 1018 (1989).
[16] M. Slack, *Combust. Flame,* **28,** 241 (1977).
[17] M. A. Hanning-Lee, M. J. Pilling, and J. F. Warr, *J. Chem. Soc. Faraday Trans.,* **87,** 2907 (1991).
[18] J. Warnatz, in *Combustion Chemistry,* W. C. Gardiner, Ed., Springer Verlag, Berlin, 1984, p. 197.
[19] W. Tsang and R. F. Hampson, Jr., *J. Phys. Chem. Ref. Data,* **15,** 1087 (1986).
[20] J. A. Miller and C. T. Bowman, *Prog. Energy Combust. Sci.,* **15,** 287 (1989).
[21] R. Atkinson, D. L. Baulch, R. A. Cox, R. F. Hampson, Jr., J. A. Kerr, and J. Troe, *J. Phys. Chem. Ref. Data,* **21,** 1125 (1992).
[22] D. L. Baulch, C. F. Cobos, R. A. Cox, C. Esser, P. Frank, Th. Just, J. A. Kerr, M. J. Pilling, J. Troe, R. W. Walker, and J. Warnatz, *J. Phys. Chem. Ref. Data,* **21,** 411 (1992).
[23] R. J. Kee, F. M. Rupley, and J. A. Miller, *Chemkin-II: A Fortran Chemical Kinetics Package for the Analysis of Gas-Phase Chemical Kinetics,* Sandia National Laboratory, Report SAND89-8009, 1989.
[24] A. E. Lutz, R. J. Kee, and J. A. Miller, *SENKIN: A Fortran Program for Predicting Homogeneous Gas-Phase Chemical Kinetics with Sensitivity Analysis,* Sandia National Laboratory, Report SAND87-8248, 1987.
[25] R. J. Kee, F. M. Rupley, and J. A. Miller, *The Chemkin Thermodynamic Database,* Sandia Report 87-8215, 1987.
[26] J. V. Michael, *Prog. Energy Combust. Sci.,* **18,** 327 (1992).
[27] M. A. A. Clyne and B. A. Thrush, *Trans. Farad. Soc.,* 139 (1962).
[28] M. G. Bryukov, A. A. Kachanov, R. Timonnen, J. Seetula, J. Vandoren, and O. M. Sarkisov, *Chem. Phys. Lett.,* **208,** 392 (1993).
[29] M. R. Soto, M. Page and M. McKee, *Chem. Phys. Lett.,* **187,** 335 (1991).
[30] M. R. Soto, and M. Page, *J. Chem. Phys.,* **97,** 7287 (1992).
[31] I. M. Campbell and B. J. Handy, *J. Chem. Soc. Farad. Trans. I,* **75,** 2097 (1975).
[32] M. C. Lin, Y. He, and C. F. Melius, *Int. J. Chem. Kinet.,* **24,** 489 (1992).
[33] M. G. Michaud, P. R. Westmoreland, and A. Feitelberg, in *Twenty Fourth Symposium (International) on Combustion,* The Combustion Institute, Pittsburgh, Pennsylvania, 1992, pp. 879–887.
[34] M. Slack, and A. Grillo, *Combust. Flame,* 31, 275 (1978).
[35] J. B. Burkholder, A. Mellouki, R. Talukdar, and A. R. Ravishankara, *Int. J. Chem. Kinet.,* **24,** 711 (1992).
[36] W. G. Mallard, F. Westley, J. T. Herron, R. F. Hampson, and D. H. Frizzell, *NIST Chemical Kinetics Database: Version 5.0,* National Institute of Standards and Technology, Gaithersburg, Maryland, 1993.
[37] R. A Cox and R. G. Derwent, *J. Photochem.,* **4,** 139 (1975).
[38] C. J. Howard, *J. Chem. Phys.,* **67,** 5258 (1977).
[39] A. A. Jemi-Alade and B. A. Thrush, *J. Chem. Soc. Farad. Trans.,* **86,** 3355 (1990).

Received January 5, 1995
Accepted June 13, 1995